Desorption of Polycyclic Aromatic Hydrocarbons from a Soot Surface: Three- to Five-Ring PAHs

ARTICLE *in* THE JOURNAL OF PHYSICAL CHEMISTRY A · NOVEMBER 2009

Impact Factor: 2.69 · DOI: 10.1021/jp908862c · Source: PubMed

4 AUTHORS, INCLUDING:

Yuri Bedjanian
CNRS Orleans Campus
67 PUBLICATIONS **853** CITATIONS
SEE PROFILE

Alexandre Tomas
Ecole des Mines de Douai
41 PUBLICATIONS **241** CITATIONS
SEE PROFILE

Desorption of Polycyclic Aromatic Hydrocarbons from a Soot Surface: Three- to Five-Ring PAHs

Angélique Guilloteau,[†,‡] Yuri Bedjanian,*[,†] Mai Lan Nguyen,[†] and Alexandre Tomas[‡]

Institut de Combustion, Aérothermique, Réactivité et Environnement (ICARE), CNRS, 45071 Orléans Cedex 2, France and Département Chimie et Environnement, Ecole des Mines de Douai, BP 838, 59508 Douai, France

Received: September 14, 2009; Revised Manuscript Received: November 4, 2009

The kinetics of the thermal desorption of a set of three- to five-ring polycyclic aromatic hydrocarbons (PAHs) from a laboratory-generated kerosene soot surface was studied over the temperature range 250−355 K in a low-pressure flow reactor combined with an electron-impact mass spectrometer. Two methods were used to measure the desorption rate constants: monitoring of the surface-bound PAH decays due to desorption using off-line HPLC measurements of their concentrations in soot samples and monitoring of the desorbed molecules (anthracene and phenanthtrene) in the gas phase using in situ mass spectrometric detection. The Arrhenius parameters (*A* factors and activation energies) for the desorption rate constants of 10 soot-bound PAHs were determined. The PAH−soot binding energies were found to be similar for PAHs with the same number of carbon atoms and to increase with increasing number of PAH carbon atoms. The experimental data are discussed in the frame of the existing theoretical gas to particle partitioning model.

1. Introduction

Polycyclic aromatic hydrocarbons (PAHs), which principally originate from incomplete combustion and pyrolytic processes at high temperatures, are recognized as important pollutants with carcinogenic and mutagenic properties.[1] Partitioning of PAHs between particulate and gas phases is a very important factor determining the atmospheric fate of these compounds: transport, reactivity, deposition processes, as well as their health and climate impact and influence on the chemical composition of the atmosphere.[1−3]

The distribution of PAHs between the two phases depends on the physicochemical properties of PAH (saturation vapor pressure), the physicochemical properties of the particulate phase (surface area, composition), and the environmental conditions (temperature) and is usually described by a partition coefficient K_P (m^3 μg^{-1})[4−6]

$$K_P = \frac{(F/\mathrm{TSP})}{A}$$

where A and F (in ng m^{-3}) are equilibrium concentrations in the gas and particulate phase, respectively, and TSP (in μg m^{-3}) is the total suspended particulate matter.

Gas−solid adsorptive partitioning theory predicts that[5]

$$K_P = \frac{N_S a_{TSP} T\, e^{(\Delta H_{des} - \Delta H_{vap})/RT}}{1600 P_L^\circ} \quad (1)$$

where N_S is the concentration of surface adsorption sites (mol cm^{-2}), a_{TSP} is the specific surface area of the particulate matter (m^2 g^{-1}), ΔH_{des} and ΔH_{vap} are the enthalpies (kJ mol^{-1}) of desorption and vaporization, respectively, R is the molar gas constant, T is the temperature (K), and P_L° is the subcooled liquid vapor pressure (Torr). The kinetic and thermodynamic data on the desorption of PAH from solid surfaces of atmospheric relevance is almost nonexistent. Yet, ΔH_{des} is a key parameter allowing direct calculations of K_P via eq 1 for given atmospheric aerosol loading (a_{TSP}) and using tabulated physicochemical parameters (ΔH_{vap}, P_L°) of the species of interest.

The present paper is the second one in a series on a systematic study of the kinetics and thermodynamics of a large set of PAHs desorption from a kerosene soot surface carried out in our laboratory. Soot particles, being a coproduct of the incomplete combustion of fossil fuels and biomass, represent an important source of particulate PAHs. Considering that PAHs have a high affinity to carbonaceous surfaces, adsorption of PAHs onto the soot fraction of atmospheric aerosols may be an important mechanism affecting PAHs partitioning between particulate and gas phases in the atmosphere.[7] There were only a few laboratory studies dealing with the distribution of PAHs between the gas phase and the carbonaceous aerosol.[8−10] The work of Aubin and Abbatt,[10] where soot from the combustion of *n*-hexane was used as a model for atmospheric aerosols, seems to be the only one where the interaction of PAH with soot was realized with well-characterized solid support. However, it should be noted that only small PAHs (naphthalene, acenaphtylene, and acenaphtene), that is, most volatile compounds dominantly partitioned to the gas phase under atmospheric conditions, were considered.[10] In our previous paper,[11] the results from a kinetic study of the desorption of two four-ring PAHs, fluoranthene and pyrene, from soot have been reported. The experimental approach used for the study of PAHs desorption from the laboratory-generated soot samples has also been detailed. The present paper reports the results of the experimental measurements of the kinetic and thermodynamic parameters for desorption of three- to five-ring PAHs from soot.

2. Experimental Section

Preparation of Soot Samples. A flat-flame burner used for the preparation and deposition of soot samples from premixed flames of liquid fuels was described in detail previously.[11,12] It allowed for the generation of flames of high stability with a known fuel/oxygen ratio. In the present study the mixture of

* To whom correspondence should be addressed. Phone: +33 238255474. Fax: +33 238696004. E-mail: bedjanian@cnrs-orleans.fr.
† Réactivité et Environnement (ICARE).
‡ Ecole des Mines de Douai.

10.1021/jp908862c
Published on Web 11/19/2009

TABLE 1: List of Kerosene Soot-Bound PAHs Considered in the Present Study

PAH	abbreviation	detector[a]	concentration[b] (μg mg^{-1})	concentration[c] (10^{-6} mol m^{-2})
phenanthrene	Phe	F	1.90 ± 0.13	0.089
anthracene	Ant	F	0.31 ± 0.03	0.015
benzo(*ghi*)fluoranthene	BghiF	UV	0.78 ± 0.03	0.029
acepyrene	AcP	F	nc[d]	nc
benzo(*a*)anthracene	BaA	F	0.17 ± 0.01	0.006
chrysene	Chr	F	0.32 ± 0.02	0.012
benzo(*e*)pyrene	BeP	UV	0.83 ± 0.05	0.028
benzo(*b*)fluoranthene	BbF	F	0.57 ± 0.04	0.019
benzo(*k*)fluoranthene	BkF	F	0.13 ± 0.01	0.004
benzo(*a*)pyrene	BaP	F	0.92 ± 0.04	0.030

[a] F, fluorescence detector; UV, multiwavelength UV/visible detector. [b] Error represents one standard deviation from mean value from five replicates. [c] Calculated using specific surface area of 120 m^2 g^{-1}.[12] [d] nc, not calibrated.

hydrocarbons (decane:propylbenzene:propylcyclohexane = 74:15:11) was used as the fuel. This mixture, which is referred to as kerosene in the paper, was chosen as a proxy of kerosene as it well represents the combustion of kerosene and, from another side, facilitates soot preparation due to a smaller number of hydrocarbon constituents (with lower boiling point) compared with kerosene. Soot particles from stabilized premixed flames with a richness near 2.0 (the fuel/oxygen ratio multiplied by stoichiometric coefficient of oxygen) were sampled at 4 cm above the burner surface and deposited on the outer surface of a cylindrical Pyrex tube (0.9 cm o.d.), which was rotated and moved through the flame. In order to minimize the influence of thermal fluctuations on the concentrations of soot-bound PAHs and to ensure a reproducible PAHs content of the collected soot, the support tube was thermostabilized by circulating thermostatted (45 °C) water inside this tube.[11] In a series of specific test experiments, where the influence of combustion and soot deposition conditions on soot PAHs content was studied,[11] it was shown that this procedure of soot sample preparation provided soot samples with highly reproducible concentrations of PAHs.

Flow Reactor. The kinetics of soot-bound PAHs desorption was studied in a flow reactor combined with a modulated molecular beam mass spectrometer for detection of gaseous species.[11,12] The main reactor consisted of a Pyrex tube (45 cm length and 2.4 cm i.d.) with a jacket for the thermostatted liquid circulation (water or ethanol). Desorption experiments were carried out using a coaxial configuration of the flow reactor with a movable triple central injector:[11,12] a Pyrex tube with deposited soot sample was introduced into the main reactor along its axis. The inner tube of the movable injector was used to provide a circulation of the thermostatted liquid inside the tube with soot sample. This allowed maintaining the same temperature in the main reactor and on the soot surface during the measurements of the PAHs desorption rate as a function of temperature.

Kinetic measurements consisted of monitoring the concentrations of PAHs adsorbed on the soot surface as a function of desorption time (residence time in the reactor) upon introduction of the soot sample into the reactor (at total pressure of 0.5−1.0 Torr of He). Two methods were used for monitoring the kinetics of particulate PAHs desorption. The first one (used for all studied PAHs) consisted in HPLC off-line concentration measurements of PAHs present in solvent extractions of soot samples corresponding to different desorption times. The second approach used in situ monitoring of the PAHs desorption kinetics by mass spectrometry with direct detection of the PAH molecules released into the gas phase from the soot surface. The application of this method in the present study was limited to the lightest PAHs (anthracene and phenanthrene) and to measurements of their high desorption rates only. Mass restriction is caused by the very low saturation vapor pressure and sticky nature of the desorbed heavier PAHs and consequent difficulties in their transportation to the ion source of the mass spectrometer in the configuration used in the present study. The limitations of this method concerning the measurements of the low desorption rates of soot-bound anthracene and phenanthrene are due to low (below detection limit) concentrations of these PAHs in the gas phase when desorption (and the rate of their release into the gas phase) is slow.

Extraction and Analysis of Particulate PAHs. For extraction of PAHs from soot samples we employed the ultrasonic-assisted extraction method[11] using a high-intensity ultrasonic processor (Sonics VC750) combined with a sonotrode of 3 mm diameter to transmit the ultrasound into the liquid. The sample extraction with an ultrasonic processor is significantly faster compared with traditionally used an ultrasonic bath due to the higher and focused energy at the probe tip. The extractions were performed in a pulsation regime with sonication and relaxation cycles of 4 and 10 s, respectively, and 3 min of total sonication time. The pulse function permits avoiding excessive heating of the solvent. Acetonitrile was found to be the most appropriate solvent[11] for PAHs extraction from soot and used throughout the present study. Analysis of the extraction efficiency has shown that the employed method provided the extraction of at least 90% of extractable concentrations of PAHs.[11]

Soot solvent extracts were separated from soot particles using Teflon filters with a pore diameter of 0.2 μm and analyzed for PAHs content using a Jasco high-performance liquid chromatograph. After injection of 20 μL of extract, compounds were separated on a 4.6 mm reverse-phase C18 column (Uptispere 5TF, Interchim) using acetonitrile/water (flow gradient) as a mobile phase at a constant flow rate of 1 mL min^{-1}. The analytical column was preceded by a 4.6 mm reverse-phase C18 guard column, and both columns were thermostatically controlled at 30 °C. PAHs were detected using multiwavelength Jasco MD-2010 UV/Visible and Jasco FP-2020 fluorescence detectors.

Particulate PAHs concentrations were quantified using calibrated solutions of PAHs mixtures. It was observed that the response of the two detectors used (fluorescence and UV/vis detectors) to the concentration of PAHs was linear in the range of PAHs concentrations used in this study. The PAHs studied in the present work are shown in Table 1. A near monolayer coverage of soot samples with PAHs was estimated in our previous study.[11]

3. Results and Discussion

PAHs Desorption Under Ambient Conditions. Fresh soot samples were used in all kinetic experiments. A series of

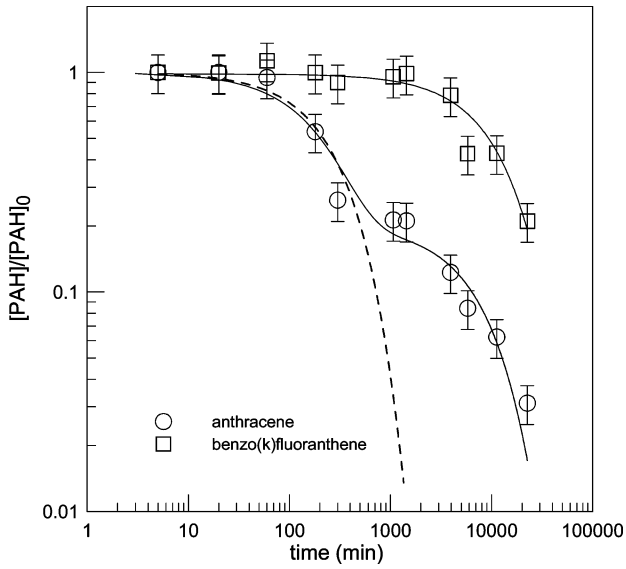

Figure 1. Examples of kinetics of soot-bound PAHs desorption under ambient laboratory conditions.

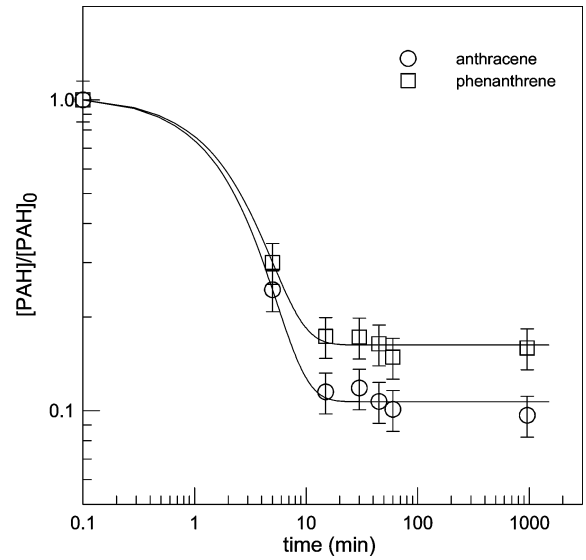

Figure 2. Kinetics of soot-bound anthracene and phenanthrene desorption measured in the low-pressure flow reactor at long desorption times (T = 300 K). The solid lines correspond to the plateau-approaching exponential fit to the experimental data.

experiments was performed to verify the chemical stability of soot samples or, more precisely, an absence of significant changes of the PAHs surface concentrations (due to desorption or photochemical degradation) during soot sample handling (10−20 min) between its preparation and introduction into the flow reactor. In these experiments the evolution of the chemical composition (PAHs abundance) of the soot was studied as a function of soot residence time under ambient laboratory conditions (atmospheric pressure, $T = 298 \pm 3$). Examples of the kinetics observed for decays of soot-bound PAHs concentrations are shown in Figure 1. Solid lines represent the best fit to the experimental data with exponential and biexponential functions, respectively, for benzo(*k*)fluoranthene and anthracene. The dashed line, which is an exponential fit to anthracene data, shows that these data cannot be approximated by a single-exponential function. Analysis of the biexponential fit shows that the desorption rate of 80% of the anthracene molecules initially present on the soot surface is a factor of 50 higher than that of the remainder 20%. One of the possible reasons for this behavior is an inhomogeneity of the soot surface or, in other words, the existence of at least two different types of sorption sites. Another reason for this retarded desorption of PAHs can be their trapping in soot pores due to slow diffusion and the readsorption process.

It should be noted that the results presented in Figure 1 have a qualitative character as the rate of surface PAHs decay in these experiments is influenced by several processes: thermal desorption, possible PAHs photodegradation (soot samples were exposed day and night), and slow (at atmospheric pressure) diffusion of desorbed PAHs through the soot sample accompanied with PAHs readsorption, which could limit the rate of PAHs release into the gas phase. What is important in the context of the experimental protocol of the kinetic measurements in the present study is that the concentrations of particulate PAHs in freshly prepared soot samples do not undergo significant changes during up to 1 h exposure under ambient laboratory conditions (even for the lightest compounds, phenanthrene and anthracene, considered in this study).

Measurements of PAHs Desorption Rate. Examples of the kinetics of particulate anthracene and phenanthrene desorption measured in a flow reactor at long residence times and low pressure (≤0.1 Torr of He) with HPLC detection of the species are shown in Figure 2. An important observation is that the kinetics are reaching a plateau, that is, a part of sorbed PAHs is remaining on the soot surface and is not released into the gas phase even at fairly long pumping times (near 17 h). A similar effect was also observed for heavier compounds at higher temperatures. Some experiments focused on this noncomplete PAHs desorption have been carried out in our previous study.[11] It was observed that (i) the number of PAHs molecules remaining on the surface (plateau level) decreases with increasing temperature, and (ii) PAH are desorbing homogeneously from the soot surface, and the concentration of the nondesorbed PAH molecules is similar throughout the soot sample volume. The PAHs trapping in the pores of soot samples due to slow diffusion retarded by PAHs readsorption was proposed as the most probable reason for this noncomplete desorption of PAHs.

In the present work, as in our previous study,[11] the undesorbed molecules were not considered in calculations when determining the desorption rate constants. At low desorption rates the experimental data could be reasonably described by first-order kinetics. In this case, the first-order rate coefficients were determined from the exponential fits to the experimental points

$$[\mathrm{PAH}] = [\mathrm{PAH}]_0 \times \exp(-k_{\mathrm{des}}t)$$

When the existence of a plateau was necessary to be taken into account the kinetics were fitted with an exponential function approaching the plateau

$$[\mathrm{PAH}] = [\mathrm{PAH}]_{\mathrm{plateau}} + ([\mathrm{PAH}]_0 - [\mathrm{PAH}]_{\mathrm{plateau}}) \times \exp(-k_{\mathrm{des}}t) \quad (2)$$

where $[\mathrm{PAH}]_0$, $[\mathrm{PAH}]$, and $[\mathrm{PAH}]_{\mathrm{plateau}}$ are particulate PAH concentrations at $t = 0$, t, and the plateau region, respectively.

In order to ensure the correct measurements of the rate constants of the soot-bound PAHs desorption, the experimental conditions should be carefully chosen to avoid the secondary process of PAHs readsorption to the soot surface. This issue was a subject of specific experiments in our previous study.[11] It was shown that the rate of PAHs readsorption could be minimized by an increase of the flow rate in the reactor (leading, at a given pressure, to lower gas-phase PAH concentrations) and/or a decrease of the total mass of the soot sample (equivalent

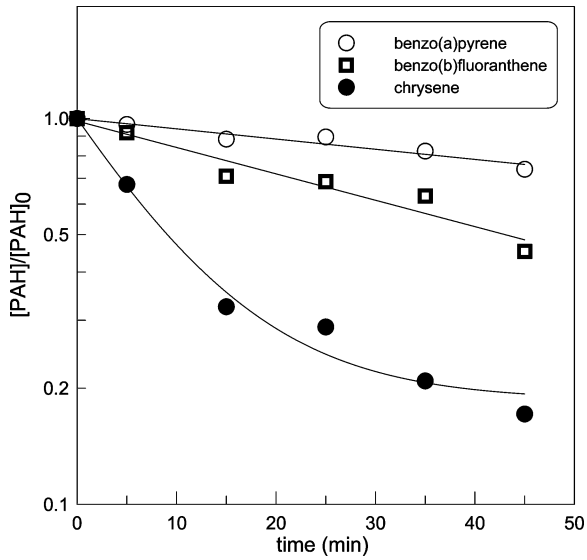

Figure 3. Desorption kinetics of soot-bound benzo(*a*)pyrene, benzo(*b*)fluoranthene, and chrysene at $T = 325$K.

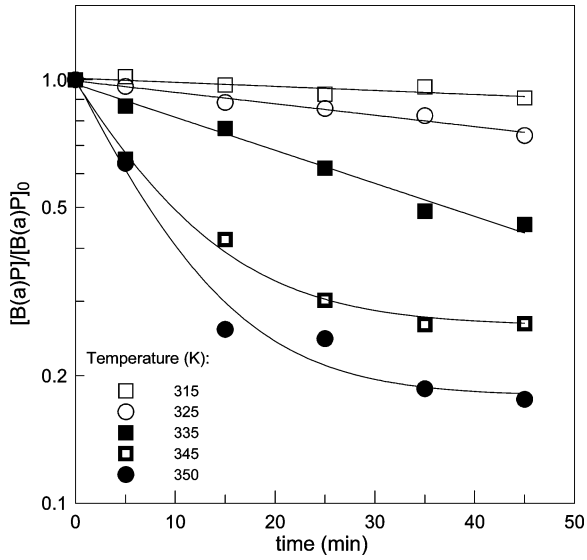

Figure 4. Kinetics of soot-bound benzo(*a*)pyrene desorption at different temperatures.

to a decrease of the initial number of particulate PAH molecules). It was shown that the possible influence of the PAHs readsorption process can be neglected under experimental conditions for which the values of the empirical parameter representing the flow rate (in cm s^{-1}) to soot sample mass (in mg) ratio are higher than 6000 cm s^{-1} mg^{-1}. In the present experiments, this requirement was respected, flow rates and soot sample masses being in the ranges 3000−4300 cm s^{-1} and 0.2−0.5 mg, respectively.

PAHs Desorption Rate as a Function of Temperature. Examples of kinetic runs for desorption of different compounds measured at a fixed temperature in the reactor ($T = 325$ K) are shown in Figure 3. As one could expect, the heavier the PAH molecule, the lower the desorption rate. Figure 4 shows examples of kinetic runs for desorption of benzo(*a*)pyrene from the soot surface measured at different temperatures. Continuous lines represent the simple exponential ($T = 315$, 325, and 335 K) or plateau-approaching exponential ($T = 345$ and 350 K, according to eq 2) function fits to the experimental data that were used to derive the values of the desorption rate constant

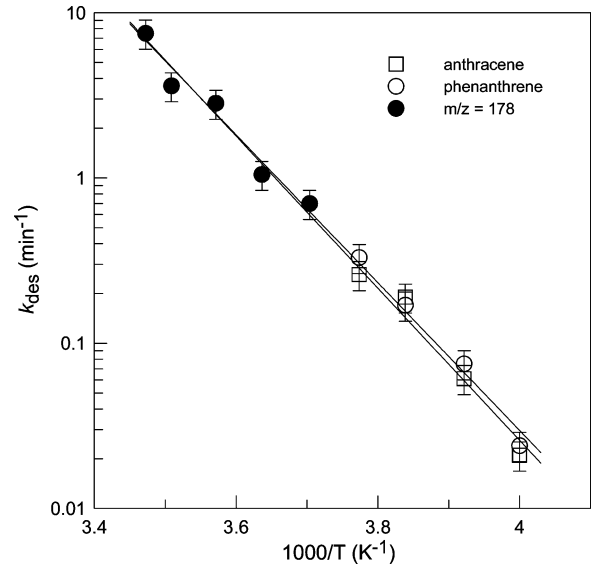

Figure 5. Temperature dependence of the desorption rate constants of soot-bound phenanthrene and anthracene: (open symbols) data from off-line HPLC separate detection of the particulate phenanthrene and anthracene; (filled circles) data from gas-phase mass spectrometric monitoring of the desorbed species at $m/z = 178$ (see text).

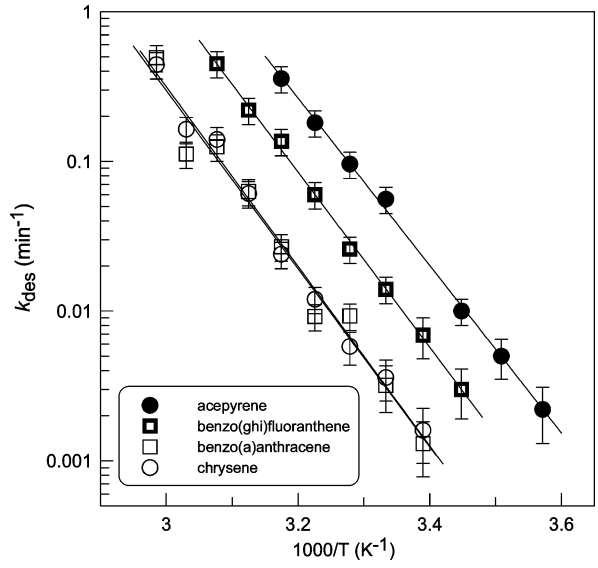

Figure 6. Temperature dependence of the desorption rate constants of soot-bound acepyrene, benzo(*ghi*)fluoranthene, benzo(*a*)anthracene, and chrysene.

(k_{des}) at different temperatures. The experimental uncertainty on the procedure of the determination of k_{des} was estimated to be within 15−25%. However, it could be much higher (up to 50%) for the lowest desorption rates measured (corresponding to a few percent decrease of the particulate PAH concentration).

The temperature dependence of the desorption rate constant was described by the Arrhenius equation

$$k_{des} = A \times \exp(-E_A/RT)$$

where A is the pre-exponential frequency factor, E_A is the activation energy for desorption, and R is the molar gas constant. Temperature dependences of k_{des} observed for the different compounds studied are shown in Figures 5−7, where continuous lines represent the best Arrhenius expression fit to the experimental data.

Considering the data for anthracene and phenanthrene presented in Figure 5, one can note good agreement and comple-

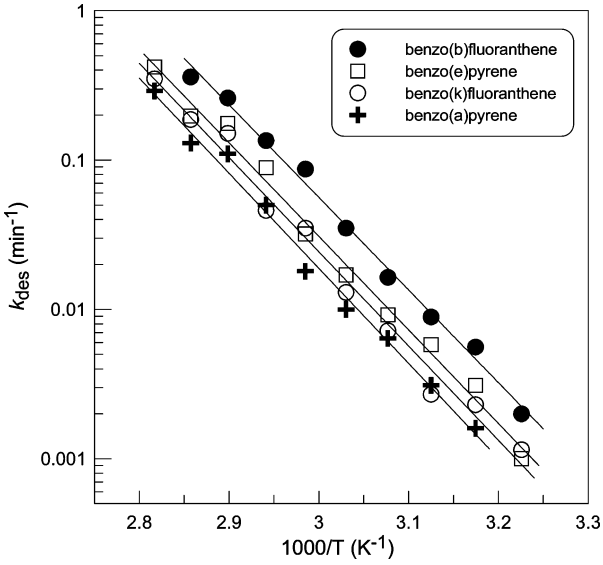

Figure 7. Temperature dependence of the desorption rate constants of soot-bound benzo(*b*)fluoranthene, benzo(*e*)pyrene, benzo(*k*)fluoranthene, and benzo(*a*)pyrene. Uncertainties on k_{des} (similar to those in Figure 6) are not shown for simplicity.

mentarities of the results obtained by two different approaches used for the measurements of k_{des}: off-line analysis of the particulate PAHs concentrations (slow desorption) and in situ mass spectrometric detection of the desorbed PAHs in the gas phase (rapid desorption). In the latter case, the desorption of phenanthrene and anthracene was studied by monitoring by mass spectrometry the sum of their concentrations in the gas phase (sum of peak intensities at $m/z = 178$). The study of the desorption kinetics of these two species using the sum of their relative concentrations is justified since the desorption rate constants of these two PAHs are similar within experimental uncertainty (Figure 5). The desorption rate constants were determined using gas-phase kinetic profiles for desorbed PAHs in accordance with the following expression for the number of PAHs molecules desorbed from the soot surface, Δ[PAH]

$$\Delta[\mathrm{PAH}] = [\mathrm{PAH}]_0 - [\mathrm{PAH}] = [\mathrm{PAH}]_0 \times (1 - \exp(-k_{des}t))$$

where $[\mathrm{PAH}]_0$ and [PAH] are the concentrations of particulate PAHs corresponding to desorption times 0 and t, respectively, which could be calculated by integration of the gas-phase kinetic profiles detected at $m/z = 178$.[11]

TABLE 2: Results of the Experiments on Desorption of PAHs from the Soot Surface[a]

PAH	Structure	Molecular weight (g mol^{-1})	T-range (K)	[b] A (10^{15}s^{-1})	[c] E_A (kJ/mol)
Phe		178	250 - 290	0.4 (4)	85.6 ± 2.8
Ant	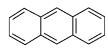	178	250 - 290	1.1 (4)	88.1 ± 3.2
Fla		202	260 - 320	0.4 (2)	93.9 ± 1.7
Pyr		202	260 - 320	0.6 (2)	95.2 ± 1.8
BghiF		226	290 - 325	7.7 (2)	112.1 ± 1.9
AcP		226	280 - 315	3.5 (2)	107.1 ± 1.9
BaA	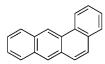	228	295 - 335	3.5 (14)	113.9 ± 6.9
Chr	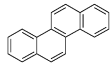	228	295 - 335	5.3 (5)	114.9 ± 3.9
BeP		252	310 - 355	3.2 (4)	119.9 ± 4.1
BbF	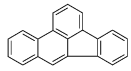	252	310 - 350	3.7 (4)	118.7 ± 3.5
BkF	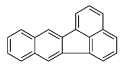	252	310 - 355	3.4 (6)	120.8 ± 4.9
BaP	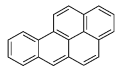	252	315 - 355	3.9 (5)	121.8 ± 4.4

[a] Data for Fluoranthene (Fla) and Pyrene (Pyr) are from ref 11. [b] Shown in parentheses is the uncertainty factor on the measured values of A. [c] The quoted error represents 1σ statistical uncertainty.

TABLE 3: Thermodynamic Parameters of Selected PAHs Studied: Present Work and Literature Data

PAH	ΔH_{des} (kJ mol^{-1})[a]	ΔH_{sub} (kJ mol^{-1})[b]	ΔH_{vap} (kJ mol^{-1})[c]	$\Delta H_{des} - \Delta H_{vap}$ (kJ mol^{-1})
Phe	85.6	88.9	76.2	9.4
Ant	88.1	99.7	76.6	11.5
Fla	93.9	98.3	85.4	8.5
Pyr	95.2	97.9	86.7	8.5
BaA	113.9	115.5	99.2	14.7
Chr	114.9	118.8	99.7	15.2
BeP	119.9	117.9	110.5	9.4
BbF	118.7	119.2	109.2	9.5
BkF	120.8	130	109.2	11.6
BaP	121.8	122.5	110.9	10.9

[a] This study, except fluoranthene and pyrene:[11] $\Delta H_{des} = E_A$. [b] Nass et al.,[23] except benzo(*k*)fluoranthene.[24] [c] Yamasaki et al.[25]

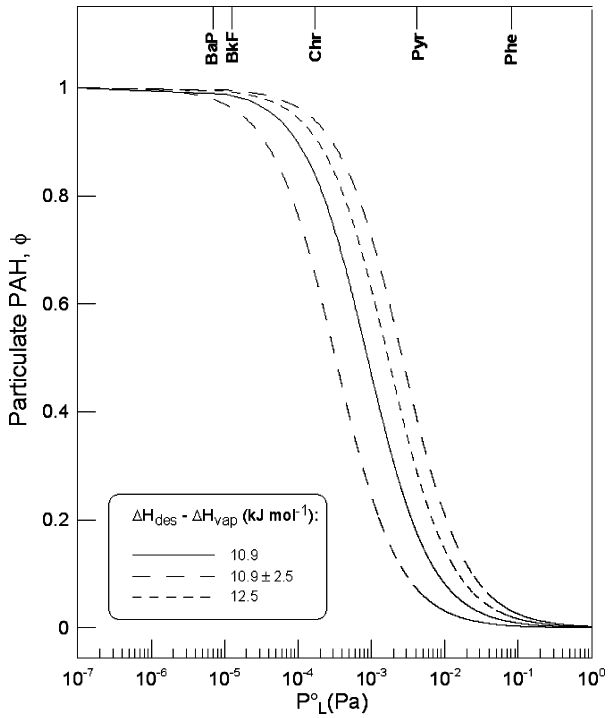

Figure 8. Fraction of PAHs adsorbed on the particulate matter (ϕ) as a function of PAHs subcooled liquid vapor pressure, calculated for different values of $\Delta H_{des} - \Delta H_{vap}$.

The resulting Arrhenius parameters determined for all compounds studied are summarized in Table 2. One can note that the temperature range of the measurements is different for different compounds. In fact, the *T* range was defined by the condition of the measurability of the PAH desorption rate under the experimental conditions used (monitoring time of the desorption kinetics from a few minutes to 1 h). Another observation is that the results obtained for the pre-exponential factors are not very sensitive to the experimental data and are therefore determined with high uncertainty.

As one would expect, a trend in the ordering of PAHs with respect to the desorption thermodynamics is observed: desorption energies (which are equivalent to the binding energies for a nonactivated desorption) are very close for PAHs with the same number of carbon atoms and increase with increasing number of PAHs carbon atoms. This trend is in line with the available literature data on PAHs desorption from carboneous materials[10,13,14] and is consistent with the additivity of the van der Waals forces which dominate the PAHs−soot interaction.

The data obtained in the present study for the desorption activation energies can be compared with the sublimation enthalpies of corresponding species (Table 3), which are relevant to binding energy for desorption from PAH multilayer coverage or when the activation energies for desorption from monolayer and multilayer coverages are similar.[15] One can note that the measured activation energies are quite close to the corresponding sublimation enthalpies. The similarity of the activation energies for PAHs desorption from the soot surface and the corresponding sublimation enthalpies seems to be consistent with the structural resemblance between PAHs and graphitic sheets of soot.

In many desorption studies the accent is put on the activation energies and the preexponential factors are usually assumed to have a "typical" value of 10^{13} s^{-1}. However, the prefactors for desorption of large molecules can be significantly higher than typical estimates for small molecules.[16] The experimental data from the present study (Table 2) seem to show a trend of the increase of *A* factor for larger PAHs molecules. An extended discussion including comparative and trend analysis of the data on Arrhenius *A* factors and activation energies of PAH desorption for a larger set of PAHs (desorption of 6-ring PAHs from soot surface is under study in our laboratory) will be presented in our next paper.

Atmospheric Implications. As already mentioned in the Introduction, for the partition coefficient K_P gas−solid adsorptive partitioning theory predicts[5]

$$K_P = \frac{N_S a_{TSP} T\, e^{(\Delta H_{des} - \Delta H_{vap})/RT}}{1600 P_L^\circ}$$

Assuming the value of $\Delta H_{des} - \Delta H_{vap}$ to be constant within a homologous series of molecules, this equation leads to a linear relationship between log K_P and log P_L°

$$\log K_P = m \times \log P_L^\circ + b$$

which has been widely used to interpret the PAHs partitioning observed under a large variety of environmental conditions (for example, see refs 17−20). The assumption of a constant value of $\Delta H_{des} - \Delta H_{vap}$ for PAH molecules is based on the field data of Yamasaki et al.[4] analyzed by Pankow[5] and, to our knowledge, has never been systematically verified. Comparing the field data of Yamasaki et al.[4] for the gas-particle distribution of atmospheric PAH with the theoretical framework and using $N_S = 4 \times 10^{-10}$ mol cm^{-2}, Pankow[5] estimated a value of near 3 kcal/mol (∼12.5 kJ/mol) for $\Delta H_{des} - \Delta H_{vap}$ for the series of PAHs. The values $\Delta H_{des} - \Delta H_{vap}$ obtained in the present study for 10 PAHs are in the range 8.5−15.2 kJ mol^{-1} (Table 3) with a mean value of 10.9 ± 2.5 kJ mol^{-1}. These data can be compared with those of Yamasaki et al. (8.3−16.7 kJ mol^{-1})[4] and those of Aubin and Abbatt (13−17 kJ mol^{-1}),[10] measured for ethylbenzene and three two-ring PAHs. They seem to support (at least for PAHs molecules) the widely used assumption that the value of $\Delta H_{des} - \Delta H_{vap}$ can be considered to be constant within a homologous series of molecules.

The data on $\Delta H_{des} - \Delta H_{vap}$ can be applied to calculate the fraction of the total atmospheric concentration of PAHs adsorbed on the particulate matter (ϕ) using the equation originally proposed by Junge[21]

$$\phi = \frac{c_J \theta_J}{P_L^\circ + c_J \theta_J}$$

where θ_J is the concentration of the aerosol surface area (cm^2 cm^{-3}) and c_J is the compound- and temperature-dependent constant given by Pankow[5]

$$c_J = 760RTN_S e^{(\Delta H_{des} - \Delta H_{vap})/RT}$$

Figure 8 shows the results of such calculations at $T = 300$ K with $\theta_J = 1.1 \times 10^{-5}$ cm^2 cm^{-3} (urban conditions)[22] for $\Delta H_{des} - \Delta H_{vap} = 10.9 \pm 2.5$ (present study) and 12.5 kJ mol^{-1}.[5] In agreement with a previous study,[10] Figure 8 illustrates that (i) the most and least volatile compounds are not sensitive to the value of $\Delta H_{des} - \Delta H_{vap}$ and (ii) the predicted aerosol surface coverage is most sensitive to $\Delta H_{des} - \Delta H_{vap}$ in the case of semivolatile three- to four-ring PAH molecules. This highlights the importance of the knowledge of $\Delta H_{des} - \Delta H_{vap}$ values for correct modeling of the partitioning of semivolatile PAHs and the need for more precise laboratory data on ΔH_{des} for different solid supports of atmospheric relevance and for a large set of homologous compounds.

Acknowledgment. This study has been carried out within the program PRIMEQUAL 2 funded by the French Ministry of Ecology and Sustainable Development. A.G. is very grateful to Ecole des Mines de Douai and European Structural Funds for cofinancing her Ph.D. grant.

References and Notes

(1) Finlayson-Pitts, B. J.; Pitts, J. N. J. *Chemistry of the upper and lower atmosphere: theory, experiments and applications*; Academic Press: San Diego, 2000.

(2) Calvert, J. G.; Atkinson, R.; Becker, K. H.; Kamens, R. M.; Seinfeld, J. H.; Wallington, T. J.; Yarwood, G. *The Mechanisms of Atmospheric Oxidation of Aromatic Hydrocarbons*; Oxford University Press: New York, 2002.

(3) Bidleman, T. F. *Environ. Sci. Technol.* **1988**, *22*, 361.

(4) Yamasaki, H.; Kuwata, K.; Miyamoto, H. *Environ. Sci. Technol.* **1982**, *16*, 189.

(5) Pankow, J. F. *Atmos. Environ. (1967)* **1987**, *21*, 2275.

(6) Pankow, J. F. *Atmos. Environ., Part A: Gen. Top.* **1991**, *25*, 2229.

(7) Dachs, J.; Eisenreich, S. J. *Environ. Sci. Technol.* **2000**, *34*, 3690.

(8) Niessner, R.; Wilbring, P. *Anal. Chem.* **1989**, *61*, 708.

(9) Hueglin, C.; Paul, J.; Scherrer, L.; Siegmann, K. *J. Phys. Chem. B* **1997**, *101*, 9335.

(10) Aubin, D. G.; Abbatt, J. P. *Environ. Sci. Technol.* **2006**, *40*, 179.

(11) Guilloteau, A.; Nguyen, M. L.; Bedjanian, Y.; Le Bras, G. *J. Phys. Chem. A* **2008**, *112*, 10552.

(12) Lelievre, S.; Bedjanian, Y.; Pouvesle, N.; Delfau, J. L.; Vovelle, C.; Le Bras, G. *Phys. Chem. Chem. Phys.* **2004**, *6*, 1181.

(13) Steiner, D.; Burtscher, H. K. *Environ. Sci. Technol.* **1994**, *28*, 1254.

(14) Zacharia, R.; Ulbricht, H.; Hertel, T. *Phys. Rev. B* **2004**, *69*, 155406.

(15) Ulbricht, H.; Zacharia, R.; Cindir, N.; Hertel, T. *Carbon* **2006**, *44*, 2931.

(16) Fichthorn, K. A.; Miron, R. A. *Phys. Rev. Lett.* **2002**, *89*, 196103.

(17) Gustafson, K. E.; Dickhut, R. M. *Environ. Sci. Technol.* **1997**, *31*, 140.

(18) Simcik, M. F.; Franz, T. P.; Zhang, H.; Eisenreich, S. J. *Environ. Sci. Technol.* **1998**, *32*, 251.

(19) Ngabe, B.; Poissant, L. *Environ. Sci. Technol.* **2003**, *37*, 2094.

(20) Sitaras, I. E.; Bakeas, E. B.; Siskos, P. A. *Sci. Total Environ.* **2004**, *327*, 249.

(21) Junge, C. E. Basic considerations about trace constituents in the atmosphere as related to the fate of global pollutants. In *Fate of pollutants in the air and water environments*; Suffet, I. H., Ed.; John Wiley: New York, 1977; p 7.

(22) Bidleman, T. F.; Harner, T. Sorption of persistent organic pollutants to aerosols. In *Estimating Chemical Properties for the Environmental and Health Sciences, A Handbook of Methods*; Mackay, D., Boethling, R. S., Eds.; Lewis Publishers: Chelsea, MI, 2000; p 233.

(23) Nass, K.; Lenoir, D.; Kettrup, A. *Angew. Chem., Int. Ed. Engl.* **1995**, *34*, 1735.

(24) Shiu, W.-Y.; Ma, K.-C. *J. Phys. Chem. Ref. Data* **2000**, *29*, 41.

(25) Yamasaki, H.; Kuwata, K.; Kuge, Y. *Nippon Kagaku Kaishi* **1984**, 1324.

JP908862C